

# Physicochemical and Structural Characterization of Alkali-Treated Biopolymer Sphingan WL Gum from Marine *Sphingomonas* sp. WG

Jieying Lin, Jinfeng Deng, Zhenyin Huang, Hanyu Dong, Aiping Chang,\* and Hu Zhu\*

Cite This: *ACS Omega* 2023, 8, 7163–7171

Read Online

ACCESS |



Metrics &amp; More

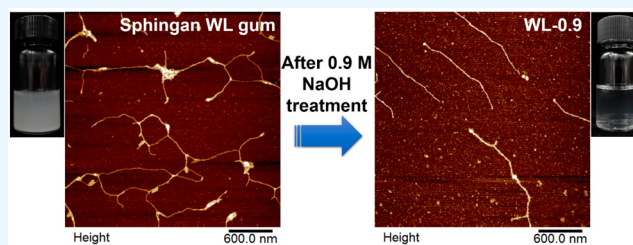


Article Recommendations



Supporting Information

**ABSTRACT:** Sphingan WL gum (WL), a kind of exopolysaccharide, is produced by *Sphingomonas* sp. WG, which was screened from sea mud samples of Jiaozhou Bay by our group. The solubility of WL was investigated in this work. First, 1 mg/mL of WL solution was stirred at room temperature for at least 2 h to obtain a uniform opaque liquid, and further the solution became clear with the increased NaOH and stirring time. Subsequently, the structural features, solubility, and rheological properties of WL before and after alkali treatment were compared systematically. FTIR, NMR, and zeta potential results indicate that the alkali causes acetyl group hydrolysis and carboxyl group deprotonation. XRD, DLS, GPC, and AFM results suggest that the alkali destroys the ordered arrangement and inter- and intrachain entanglement of polysaccharide chains. In the same case, 0.9 M NaOH-treated WL presents better solubility (stirring for 15 min to obtain a clarified solution) but, unsurprisingly, worsens rheological properties. All results demonstrated that the good solubility and transparency of alkali-treated WL will help promote its postmodification and application.



## INTRODUCTION

The solubility of naturally occurring polysaccharides, especially with water as the solvent, is important for their industrial and pharmaceutical applications.<sup>1,2</sup> In general, the structural features of polysaccharides, such as molecular weight, composition, linkage, configuration, degree of branching, and charging properties, synergistically determine their solubility (here, the focus is on aqueous solution). Cellulose, for example, has a regular (1→4)- $\beta$ -D-glucan chain (linear structure).<sup>2</sup> The intra- and intermolecular hydrogen bond (due to multi-OH groups) and interaction (owing to van der Waals' forces) form high crystalline regions; thus, natural cellulose is insoluble in water. Lowering the molecular weight and introducing branching (e.g., hydroxy propyl cellulose) or charged groups (e.g., carboxymethyl cellulose) enhance the solubility of cellulose. In addition, gum arabic is an excellent water-soluble polysaccharide because of its high branching degree, negatively charged groups (carboxy), and flexible 1→6 linkages.<sup>3</sup> Sphingan WL gum (WL), a kind of exopolysaccharide, is produced by *Sphingomonas* sp. WG (CCTCC No: M2013161), which was screened from sea mud samples of Jiaozhou Bay by our group.<sup>4,5</sup> As reported, WL is primarily composed of D-mannose, D-glucose, L-rhamnose, glucuronic acid, and O-acetyl groups, which is roughly consistent with welan gum,<sup>6,7</sup> and the molar ratio of the three neutral sugars is 1:2.28:2.12. The proposed structure is  $\alpha$ -L-Rha-(1→4)- $\beta$ -L-Rha-(1→4)- $\beta$ -D-Glc-(1→3)- $\alpha$ -D-Glc with a  $\beta$ -D-Man substituent at the third glucose residue and carboxyl and O-acyl groups. It is these branches and charged groups that give WL an acceptable water solubility. Surprisingly, we found that WL

has better rheological properties and higher oil recovery than commercial welan gum.<sup>8</sup> On the other hand, a citric acid cross-linked WL hydrogel dressing was prepared and preliminarily evaluated.<sup>9</sup> The structural characters of the produced WL were as follows:  $M_w = 2.80 \times 10^7$  Da, PDI = 2.15, glucuronic acid content = 11.30%, acetyl group content = 8.49%, crystallinity = 1.48%. Notably, at 1 mg/mL, the WL solution should be stirred by a magneton at room temperature for at least 2 h to obtain a uniform but nonclarified (milky white) liquid (Figure 1). To facilitate postmodification (functional macromolecules or small molecules react covalently with existing carboxyl or hydroxyl groups), realize visualization, and then broaden the application (food or biomedicine, for instance), it is necessary to improve the solubility of WL. Undoubtedly, WL of various molecular weights can be produced by regulating fermentation conditions or lyase (WelR) degradation, and the low molecular weight has good solubility.<sup>10</sup> This study aims to investigate the dissolution of WL with high molecular weight.

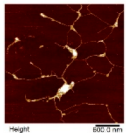
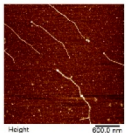
It is well-known that alkaline could break down the hydrogen bonds between polysaccharide molecules, resulting in the molecule–water interactions being greater than the molecule–molecule interactions so that polysaccharides can be

Received: January 10, 2023

Accepted: February 1, 2023

Published: February 8, 2023



	WL	WL-0.9
<sup>a</sup> $M_w$	$2.80 \times 10^7$ Da	$2.70 \times 10^7$ Da
<sup>a</sup> PDI	2.15	2.71
<sup>b</sup> Glucuronic acid content	11.30%	18.32%
	-COOH(Na)	-COONa
<sup>c</sup> Acetyl content	8.49%	-
<sup>d</sup> Crystallinity	1.48%	-
Conformation (AFM 0.01 mg/mL)		
Water solubility (10 mg+10 mL)		

**Figure 1.** Structural features and water solubility of sphingan WL gum (WL) and 0.9 M NaOH-treated WL (WL-0.9). <sup>a</sup>Determined by GPC. <sup>b</sup>Determined by the sulfuric acid-carbazole method. <sup>c</sup>Determined by the alkaline hydroxylamine method. <sup>d</sup>Calculated from XRD patterns.

dissolved in water. Sodium hydroxide (NaOH), the most common industrial alkali, has been widely used for extraction (e.g., D-glucans from edible mushrooms) and dissolution of polysaccharides (e.g., cellulose).<sup>11–13</sup> Moreover, alkali treatment will cause hydrolysis of hydrophobic acetyl groups and deprotonation of carboxylic acid groups, leading to an increased interaction between sugar chain molecules and water, which may also contribute to the enhancement of WL solubility.<sup>14,15</sup> Besides, the modification of water-soluble small or large molecules onto insoluble biopolymers can also improve their water solubility. For example, chemical modification methods of chitosan have been reviewed in many kinds of literature.<sup>16,17</sup> They indicate that chemical modification is a very necessary process to improve the water solubility of chitosan. For WL with acetyl and carboxylic groups, the relatively simple and potentially effective alkali treatment is worth trying first. Based on the above, NaOH treatment becomes the preferred choice. As expected, the addition of NaOH made the WL solution transparent, and the transparency increased with NaOH concentration (0.1–0.9 M). After dialysis purification and lyophilization, new polysaccharide samples were obtained and named WL-0.1, WL-0.3, WL-0.5, WL-0.7, and WL-0.9, corresponding to the concentration of the alkali treatment. Subsequently, the structural features of these alkali-treated WL samples, especially WL-0.9, were characterized in detail using a number of methods (FTIR, NMR, zeta potential, XRD, DLS, GPC, AFM, etc.). Furthermore, the water-solubility of WL-0.9 was compared with WL. The rheological properties of WL and WL-0.9 aqueous solutions were briefly tested at the end. The results show that WL-0.9 ( $M_w = 2.70 \times 10^7$  Da; PDI = 2.71; glucuronic acid content = 18.32%; acetyl group content = 0%; crystallinity = 0%) is completely deacetylated, negatively charged, amorphous, and stirred in water at room temperature for 15 min to get a transparent solution when the concentration is 1 mg/mL (Figure 1). We believe this natural soluble polysaccharide is more easily modified and has wider application scope, which is worthy of further study.

## EXPERIMENTAL SECTION

**Materials.** Sphingan WL gum (WL) was prepared in our lab by fermentation with *Sphingomonas* sp. WG (CCTCC No. M2013161), and the specific steps were available from the published literature.<sup>9</sup> The sodium hydroxide (NaOH) was analytical grade and used without further purification. Ultrapure water was used in all experiments.

**Preparation of Alkali-Treated WL.** 0.06 g of WL was added to 60 mL of water and stirred until a uniform milky liquid was obtained. The solution (1 mg/mL) was evenly divided into six bottles. Different weights of NaOH (0.04, 0.12, 0.20, 0.28, and 0.36 g) were added to each of the five bottles in sequence, and the final NaOH concentrations reached 0.1, 0.3, 0.5, 0.7, and 0.9 M, respectively. The nonalkali bottle served as the control. Immediately the mixture was stirred at room temperature with magnetons, and the timing began. After 48 h, the polysaccharides were purified by dialysis for 3 days and then freeze-dried. According to the NaOH concentration, the resultant solid samples were WL-0.1, WL-0.3, WL-0.5, WL-0.7, and WL-0.9, respectively.

The above experimental process was recorded by taking photos. In addition, during the dissolution process of WL in 0.9 M NaOH solution, part was purified by dialysis at various predetermined time points (3, 7, 12, 24, and 36 h). New polysaccharide samples were acquired by lyophilization.

**Characterizations and Measurements.** The FTIR spectra ( $4000\text{--}400\text{ cm}^{-1}$ , 64 scans) were recorded on an FT-IR spectrometer (Nicolet Is50, Thermo Fisher Scientific) by the KBr tablet method. The <sup>1</sup>H NMR spectra in DMSO-*d*<sub>6</sub> were collected on a 400 MHz NMR spectrometer (DPX400 UltraShield, Bruker). The contents of glucuronic acid and acetyl were determined by the sulfuric acid-carbazole method and the alkaline hydroxylamine method, respectively.<sup>18–20</sup> Acetylcholine chloride and glucuronide acid were chosen as the standard. The detailed procedures were referred to in the published literature.<sup>4</sup> The standard curves are shown in Figures S3 and S4. Dynamic light scattering (DLS) and zeta potential were measured at 25 °C using a nanoparticle size and zeta potential analyzer (Zetasizer Nano ZSE, Malvern). The X-ray diffraction profiles were measured with an X-ray diffractometer (X'Pert PXR, Panalytical) using a CuK $\alpha$  radiation at 40 kV and 40 mA. The diffraction angle ranged from 5 to 60°. The molecular weight was detected by gel permeation chromatography (GPC) using Waters 2695 high-performance liquid chromatography equipped with a 2410 refractive index detector. The column was Ultrahydrogel Linear 300 mm  $\times$  7.8 mmid. The mobile phase was 0.1 mol/L sodium nitrate at a flow rate of 0.5 mL/min at 40 °C. Dextrans were used as standards. The samples were filtered with a 0.22  $\mu$ m membrane before injection. The chain conformation was characterized by an atomic force microscope (AFM) (MultiMode 8, Bruker). The silicon probe had an elastic constant of 0.4 N/m and a resonance frequency of 70 kHz. Five  $\mu$ L of 0.01 or 0.1 mg/mL polysaccharide solutions were spin-coated on mica sheets, dried naturally, and directly observed.

To test the water solubility, 10 mg of WL-0.9 or WL was added into 10 mL of water, stirred, and photographed. The morphologies of the freeze-dried samples (1 mg/mL WL and WL-0.9 solutions) were characterized by scanning electron microscope (SEM) (Regulus-8100, Hitachi) at 5 kV. All samples were sprayed with gold for 120 s before testing.

A rotated rheometer (TA Discovery DHR-2, Waters) was used to measure the rheological properties of the WL and WL-0.9 solutions (5 mg/mL) at room temperature. The flat plate was 8 mm in diameter, and the measurement gap was 1 mm. The steady-state rheological test in Flow mode was performed with a shear rate of 0.1–100 s<sup>-1</sup>. The oscillation frequency sweep test (0.1 rad/s–10 rad/s) was conducted under a fixed strain of 1%. The relationship between the apparent viscosity and the shear rate was fitted with the following Power-law equation (eq 1)

$$\eta = k\dot{\gamma}^{n-1} \quad (1)$$

where  $\eta$  is the apparent viscosity (mPa·s);  $\dot{\gamma}$  is the shear rate (s<sup>-1</sup>);  $k$  is the consistency index; and  $n$  is the flow behavior index.

## RESULTS AND DISCUSSION

**Dissolution Process.** After stirring at room temperature for at least 2 h, 1 mg/mL of sphingan WL gum (WL) aqueous solution exhibits a homogeneous milky white liquid (Figure 2A). The transparency of the solution increases with the increase of sodium hydroxide concentration (0–0.9 M) and agitation time (0–48 h) (Figure 2B). In contrast, we found that the solution becomes absolutely clear under the

conditions NaOH concentration of 0.7 or 0.9 M and agitation time of 48 or 36 h, which indicated that the polysaccharide has been well dissolved in the water. Moreover, it was observed that the change to stirring for a long time at a lower alkali concentration could be achieved at a higher alkali concentration for a short time, suggesting that prolonged agitation time and increased alkali concentration contribute equally to the dissolution of WL under certain conditions, which may be attributed to the fact that the dissolution process is usually entropy-assisted.<sup>21</sup> To investigate the dissolution mechanism, that is, the effect of NaOH on the WL structure, these solutions were dialyzed to remove excess ions and then lyophilized and characterized. The resultant new polysaccharide samples were named WL-0.1, WL-0.3, WL-0.5, WL-0.7, and WL-0.9, corresponding to the concentration of the alkali treatment.

**Chemical Structure Analysis.** First, FTIR was used to analyze the chemical structures of polysaccharides. In the IR spectrum of WL (Figure 3A), the absorbance band at ~3400

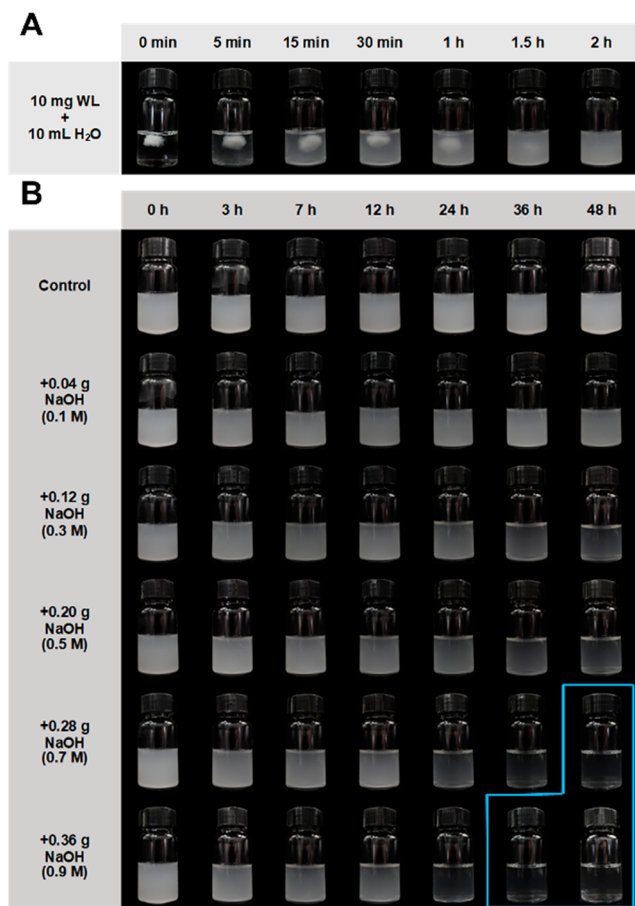


**Figure 2.** (A) Photos of the sphingan WL gum (WL) dissolution process under magneton agitation at room temperature. (B) Photos of the dissolution process of WL after adding different amounts of sodium hydroxide (NaOH) (the three samples in the blue frame are transparent).

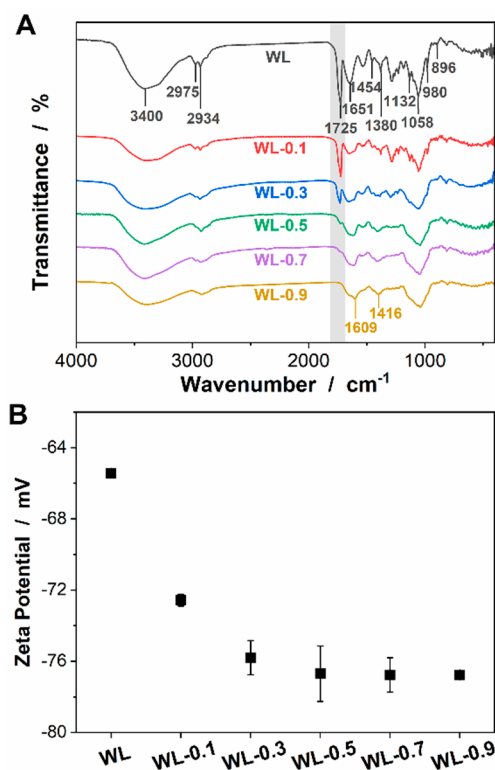


**Figure 3.** FTIR spectra (A) and zeta potentials (B) of sphingan WL gum (WL) and alkali-treated WL (WL-0.1, WL-0.3, WL-0.5, WL-0.7, and WL-0.9).

cm<sup>-1</sup> is assigned to the O–H stretching vibration, 2975 and 2934 cm<sup>-1</sup> to the C–H stretching vibration, 1725 cm<sup>-1</sup> to the C=O stretching vibration of the O-acetyl group, 1651, 1454, and 1380 cm<sup>-1</sup> to the COO<sup>-</sup> stretching vibrations, 1132, 1058, and 980 cm<sup>-1</sup> to the hydroxyl C–O stretching vibration, and 896 cm<sup>-1</sup> to the C–O–C stretching vibration at glycoside bond.<sup>9</sup> The existence of COO<sup>-</sup> groups may be due to the use of NaCl in polysaccharide purification, which causes some carboxylate groups to deprotonate. After alkali treatment, the IR characteristic bands changed significantly. In particular, the band at 1725 cm<sup>-1</sup> (acetyl C=O stretching vibration) weakens and becomes unobservable, indicating that the alkali

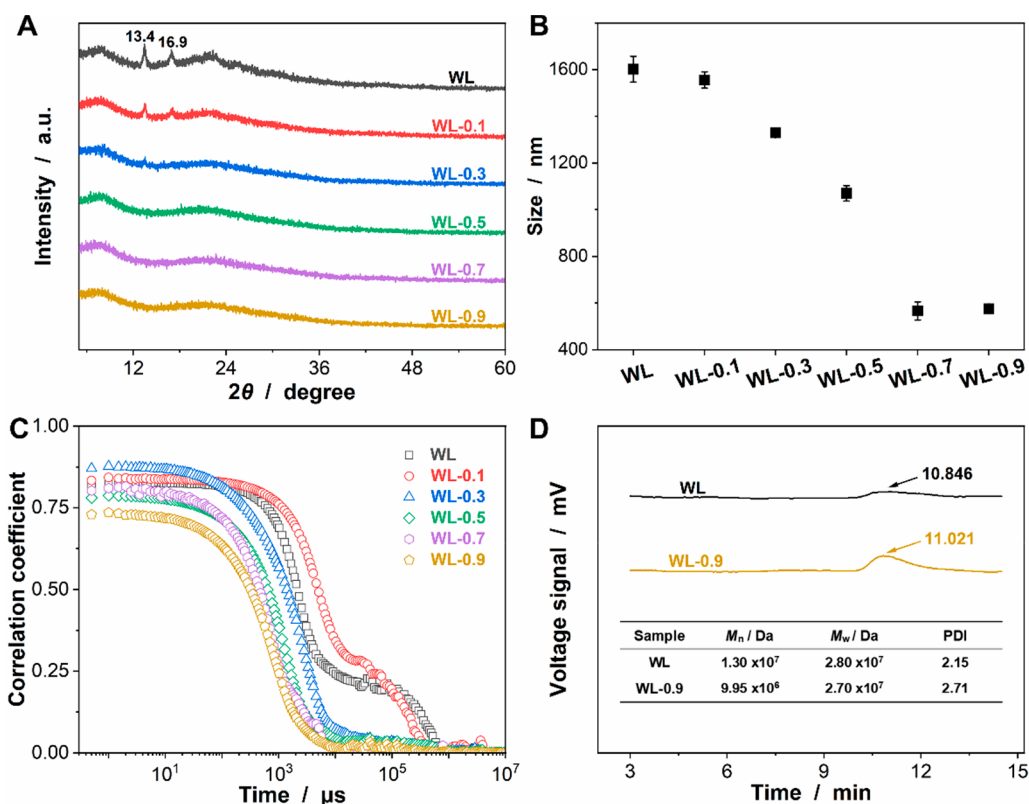


**Figure 4.** XRD patterns (A), DLS sizes (B), and DLS correlation coefficient curves (C) of spingyan WL gum (WL) and alkali-treated WL (WL-0.1, WL-0.3, WL-0.5, WL-0.7, and WL-0.9). Size values are presented as the mean  $\pm$  SD;  $n = 3$ . (D) GPC chromatograms and results (embedded table) of WL and 0.9 M NaOH-treated WL (WL-0.9).

treatment causes hydrolytic removal of acetyl groups.<sup>22</sup> Besides, the  $\text{COO}^-$  stretching vibrations occur at  $\sim 1605$  and  $\sim 1414 \text{ cm}^{-1}$  in the WL-0.9 spectrum and appear as two broad bands, revealing that the alkali treatment results in more carboxyl deprotonation.<sup>23,24</sup> It is worth noting that for the samples with fixed alkali concentration (0.9 M NaOH) and different stirring times their IR spectra show similar changes (Figure S1). Afterward, NMR and zeta potential were performed. In the  $^1\text{H}$  NMR spectrum of WL-0.9 (Figure S2), the signal belonging to the acetyl (2.07 ppm) is not present compared with the WL, indicating again that the alkali removes the acetyl groups and that there are no acetyl groups in WL-0.9.<sup>15</sup> The acetyl quantification method using acetylcholine chloride as the standard (Figure S3) also confirms the absence of acetyl groups in WL-0.9.<sup>19,20</sup> According to the sulfuric acid-carbazole method (Figure S4), the glucuronic acid content of WL-0.9 (18.32%) is  $\sim 7\%$  higher than WL (11.30%), which may be attributed to the decrease in molecular weight (due to acetyl loss) and to the increase in water solubility of WL-0.9.<sup>18</sup> Figure 3B shows that the zeta potentials of WL, WL-0.1, WL-0.3, and WL-0.5 decrease dramatically one by one and the zeta potentials of WL-0.5, WL-0.7, and WL-0.9 are all about  $-76.7 \text{ mV}$ . This again proves the progressive deprotonation of carboxyl groups and further reveals that all carboxylic acids of the last three samples have been converted to carboxylate anions.<sup>25</sup> Therefore, WL-0.9 can be said to be completely deacetylated and fully negatively charged.

**Crystallinity, Size, Molecular Weight, And Chain Conformation Analysis.** XRD is a rapid analytical technique widely used to evaluate the crystalline structure of poly-

saccharides. As illustrated in Figure 4A, a broad diffraction peak occurs at  $2\theta$  of  $\sim 20^\circ$ , indicating fibrosis of all samples.<sup>22</sup> In addition, the XRD pattern of WL shows sharp peaks at  $13.4^\circ$  and  $16.9^\circ$ , which correspond to the  $d$ -spacing of  $6.6 \text{ \AA}$ , and  $5.2 \text{ \AA}$ , demonstrating that WL has a high crystal region. The two diffraction peaks shrink after alkali treatment. WL-0.5, WL-0.7, and WL-0.9 are amorphous because no obvious peak is observed in their patterns. Based on the two narrow peaks, the crystallinity of polysaccharide was calculated by MDI Jade 6.5 software ( $2\theta = 5\text{--}60^\circ$ ). Specifically, the crystallinity of WL is  $\sim 1.48\%$ , WL-0.1 is  $\sim 1.31\%$ , and WL-0.3 is  $\sim 0.26\%$ . These values suggest that the alkali disrupts the ordered arrangement of WL and even after dialysis purification alkali-treated polysaccharide chains do not rearrange into ordered regions, which may be due to chemical structural changes such as carboxyl deprotonation (negative charge makes molecules repulsive). Similar to IR, XRD patterns of samples with fixed alkali concentration and different stirring times show the same trend as above (Figure S5).

DLS results of polysaccharide dilute solutions show that the size becomes smaller with increasing concentration of alkali treatment, and the hydrodynamic diameter of WL (1602 nm) is about 2.8 times that of WL-0.9 (575 nm) (Figure 4B). The correlation coefficient curve of WL is rough with multiple decays (Figure 4C). In contrast, the curve of WL-0.9 is smooth and a perfect anti-S shape with decreased decay time and once decay, indicating that there are polydisperse aggregates in the WL solution, but WL-0.9 disperses well in water.<sup>26,27</sup> These trends and changes suggest that the alkali treatment breaks up the intermolecular entanglement (due to hydrogen bonds or van der Waals' forces), making the treated polysaccharide

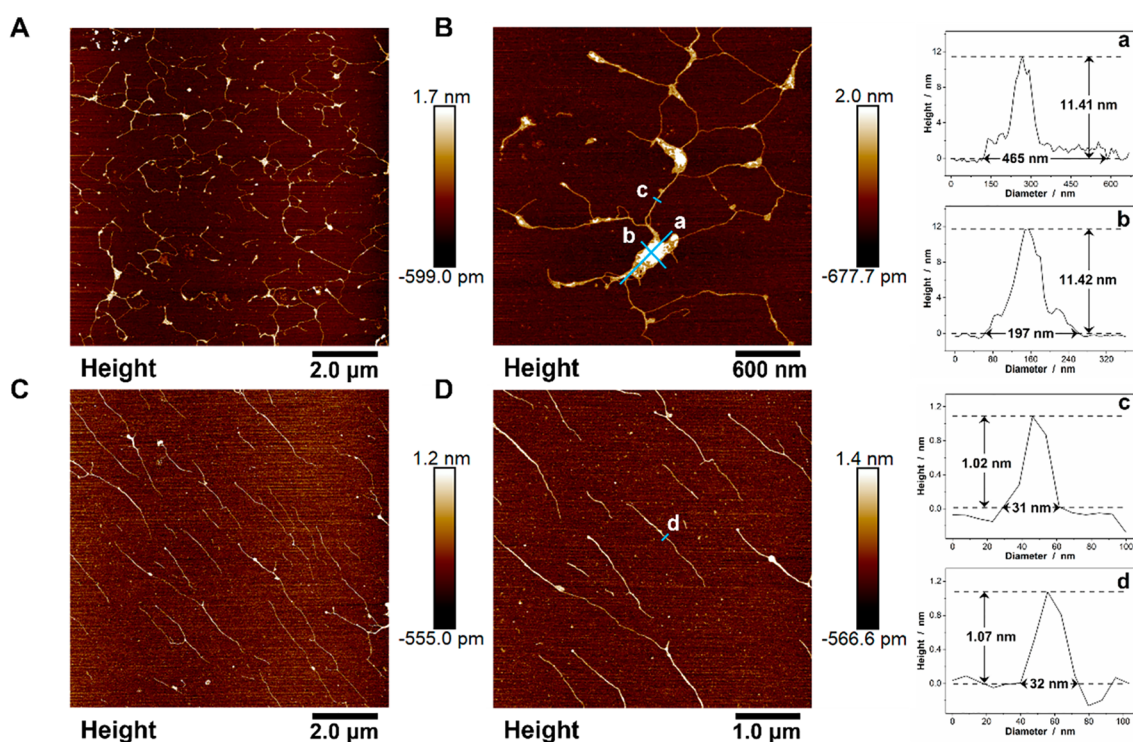


**Figure 5.** AFM images of sphingyan WL gum (WL) (A, B) and 0.9 M NaOH-treated WL (WL-0.9) (C, D) at 0.01 mg/mL. (a–d) Line profiles along the blue lines in the AFM images.

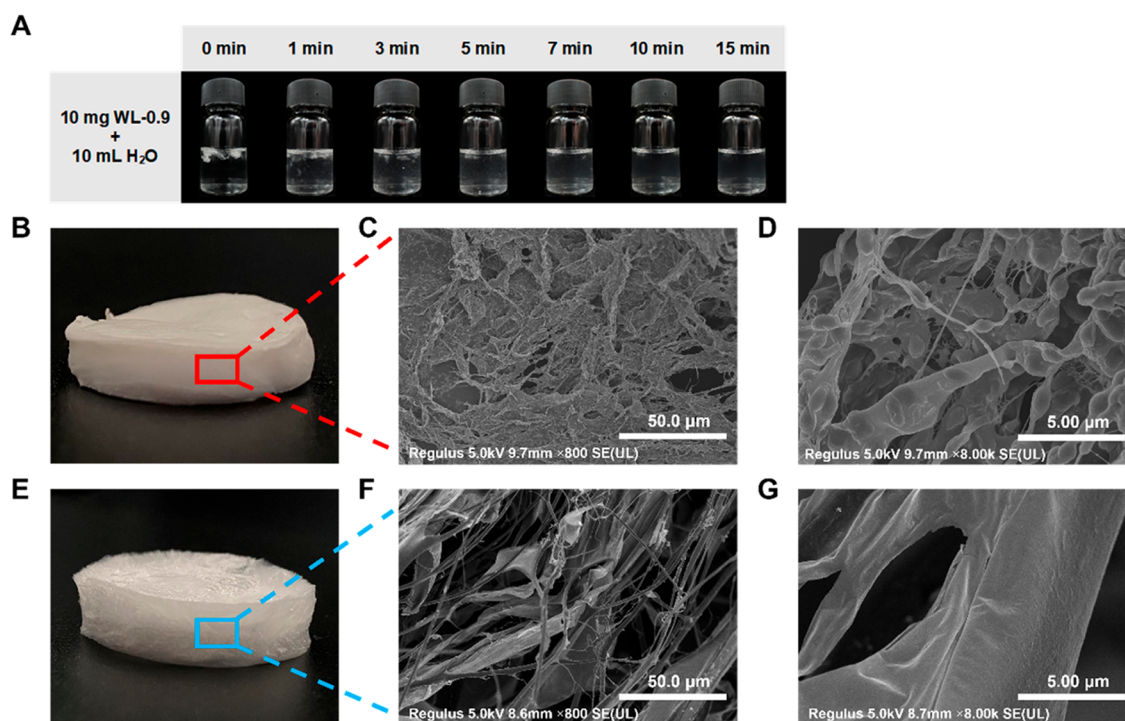


**Figure 6.** (A) Photos of the dissolution process of 0.9 M NaOH-treated sphingyan WL gum (WL-0.9) under magneton agitation at room temperature. Photo (B) and SEM images (C, D) of 1 mg/mL WL solution after lyophilization. Photo (E) and SEM images (F, G) of 1 mg/mL WL-0.9 solution after lyophilization.

better soluble in water. The GPC test determines that WL has a number-average molecular weight ( $M_n$ ) of  $1.30 \times 10^7$  Da, a weight-average molecular weight ( $M_w$ ) of  $2.80 \times 10^7$  Da, and a dispersity (PDI) of 2.15 and WL-0.9 has a lower molecular

weight ( $M_n = 9.95 \times 10^6$  Da,  $M_w = 2.70 \times 10^7$  Da) and wider polydispersity (PDI = 2.71) (Figure 4D). There are two possible reasons to explain the reduction of molecular weight and the widening of distribution after alkali treatment, one is

the removal of the acetyl group and the other is the unwinding of entanglement. However, the GPC molecular weight reduction ratio is much smaller than that of the DLS size, which is most likely because the GPC samples were filtered.

Next, the chain conformations of WL and WL-0.9 were directly observed by AFM, a visual method. In the AFM images at extremely dilute concentration (0.01 mg/mL), the WL chains exhibit polydisperse individual dendrimers with branches, nodes (inter- or intrachain entanglement), and knotted-loops (self-entanglement) (Figure 5A, B). The length, width, and height of the largest node in Figure 5B are 465, 197, and 11.41 nm, respectively (Figure 5a, b). For the thin strands, the chain height is  $0.98 \pm 0.15$  nm ( $n = 10$ , Table S1, Figure 5c), and the chain diameter is  $32 \pm 4$  nm ( $n = 10$ , Table S1, Figure 5c). In this case, the WL-0.9 is molecularly dispersed and presents the wormlike linear (Figure 5C, D), as reported for the extended chitin chains in NaOH/urea solution and the lentinan chains in water at 25 °C, suggesting that WL-0.9 is a branched rigid macromolecule.<sup>28,29</sup> Table S1 illustrates that the chain length of WL-0.9 is  $4.51 \pm 3.82$   $\mu\text{m}$  ( $n = 15$ ), indicating its polydispersity. The chain height is  $1.02 \pm 0.21$  nm ( $n = 10$ ), and the chain diameter is  $34 \pm 4$  nm ( $n = 10$ ) (Table S1, Figure 5d), which matches the thin strands of WL, implying the loss of intra- and interchain entanglement after alkali treatment. Further, these AFM parameter values are close to, but not completely consistent with, double-helical xanthan gum or triple-helical lentinan.<sup>29–31</sup> Thus, WL is thought to have an ordered helical structure, but unfortunately, the current data cannot judge how many strands a helix has. When the AFM sample concentration increases (0.1 mg/mL), as shown in Figure S6, the WL chains are arranged in parallel and entangled into a continuous network. The WL-0.9 chains become entangled, indicating that increasing concentration will cause entanglement and arrangement of polysaccharide chains.

Combined with the results of XRD, DLS, GPC, and AFM, we believe that the alkali treatment destroys the ordered arrangement and inter- and intrachain entanglement of polysaccharide molecules, thus enhancing the water solubility, and the helical structure exists before and after alkali treatment. Taking into account the changes of chemical structures, it can be assumed that acetyl removal and carboxyl deprotonation cause the polysaccharide chains to be neither entangled in a dilute solution nor assembled into ordered crystalline regions when solid.

**Solubility Properties.** Next, the water solubility of WL-0.9 was tested. Not surprisingly, WL-0.9 performed better than WL (Figure 6A vs Figure 2A). 10 mg of WL-0.9 was added to 10 mL of water and stirred for only 15 min to get a clarified solution (Figure 6A). Then the 1 mg/mL of WL and WL-0.9 were freeze-dried and observed. To the naked eye, WL looks like a white sponge (Figure 6B). SEM images of WL show a dense and thick network with a few holes and many bumps (Figure 6C, D). In contrast, WL-0.9 exhibits a sparse sponge with enhanced light transmittance (Figure 6E), and its SEM images present interlaced broad fibers with loose spacing and smooth surface (Figure 6F, G). Together with the AFM results (0.01 and 0.1 mg/mL), it is suspected that with increasing concentration, polysaccharide macromolecules are first entangled and arranged parallelly into interlinked ribbon-like fibers and then into continuous dense networks. Due to the structural characteristics, the assembly process of WL is faster than that of WL-0.9.

**Rheological Properties.** Generally, it is precisely because of the thickening and shear-thinning properties of polysaccharides that they are used in food, construction, and oil exploitation.<sup>8</sup> Therefore, the rheological properties of WL-0.9 were characterized and compared with WL. A solution of 5 mg/mL WL forms a milky white gel, which does not flow if turned upside down (Figure 7A). At the same concentration,

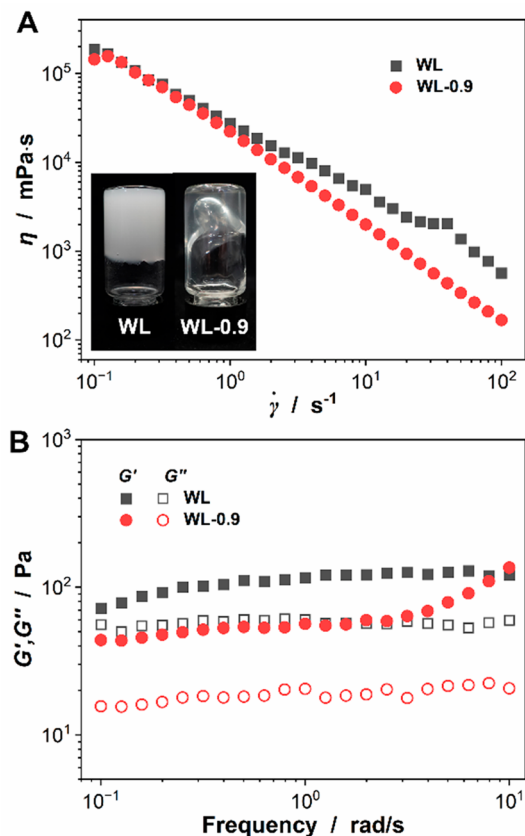


**Figure 7.** Rheological properties of sphingian WL gum (WL) and 0.9 M NaOH-treated WL (WL-0.9) (5 mg/mL). (A) Photos (embedded image) and steady shear flow curves at the shear rate of 0.1–100 s<sup>-1</sup>. (B) The storage (elastic) modulus ( $G'$ ) and the loss (viscous) modulus ( $G''$ ) curves (0.1–10 rad/s). The strain was fixed at 1%.

the WL-0.9 solution is a transparent viscous liquid that can flow. The apparent viscosity of the two samples decreases as the shear rate increases (Figure 7A), indicating that they are pseudoplastic fluids with shear-thinning behavior.<sup>32</sup> At a low shear rate, the viscosity of WL-0.9 is almost equal to that of WL; when the shear rate is 1 s<sup>-1</sup>, the apparent viscosity of WL-0.9 is  $2.21 \times 10^4$  mPa·s, and the WL is  $2.74 \times 10^4$  mPa·s. But with the increase of shear rate, the WL-0.9's viscosity begins to be lower and lower than WL. It is widely known that the disentanglement of polymer chains causes the observed shear thinning of polymer solutions during flow.<sup>33</sup> Thus, the chains in the WL-0.9 solution are considered to be more easily disentangled. The rheological parameters,  $k$  (the consistency index) and  $n$  (the flow behavior index), obtained by Power-law fitting, are listed in Table 1.<sup>34,35</sup> The  $k$  value of WL-0.9 ( $2.62 \times 10^4$ ) is 6.43% smaller than WL ( $2.80 \times 10^4$ ), and the  $n$  value of WL-0.9 (0.191) is 14.37% larger than WL (0.167). The  $n$  value of both samples is much less than 1. These imply that WL and WL-0.9 have strong pseudoplasticity, and WL-0.9 is low pseudoplastic and viscous in comparison.<sup>32–35</sup> We previously

**Table 1. Power-Law Fitting Results of Sphingan WL Gum (WL) and 0.9 M NaOH-Treated WL (WL-0.9)**

Samples	$n$	$k$	$R^2$
WL	0.167	$2.80 \times 10^4$	0.998
WL-0.9	0.191	$2.62 \times 10^4$	0.977

reported that WL's viscosity decreased with a high acetylation degree, which is different from this paper.<sup>36</sup> The reason is that the structural differences of the comparison samples in this paper are not only acetyl groups.

The storage (elastic) modulus ( $G'$ ) and the loss (viscous) modulus ( $G''$ ) were measured in oscillatory mode. As shown in Figure 7B, the  $G' > G''$  for both WL and WL-0.9, indicating the hydrogel status of the two samples.<sup>37</sup> And the two moduli of WL are not frequency-dependent in the tested frequency range, illustrating that WL exhibits a predominant solid-like behavior.<sup>38</sup> The  $G'$  of WL-0.9 shows a weak frequency dependent and shifts to higher values at high frequencies. Moreover, the  $G'$  and  $G''$  values of WL-0.9 are lower than WL on the whole. For example, at frequency 1 rad/s, the  $G'$  of WL-0.9 is 56.44 Pa, which is 51.34% lower than WL (116.00 Pa), and the  $G''$  of WL-0.9 is 20.46 Pa, which is 60.08% lower than WL (60.31 Pa). These results suggest that the viscoelasticity of WL-0.9 is worse than that of WL.

## CONCLUSIONS

In summary, 1 mg/mL of the sphingan WL gum aqueous solution was stirred at room temperature for at least 2 h to produce a milky liquid; in the same case, WL-0.9 after alkali treatment was stirred for 15 min to get a clear liquid. This phenomenon is closely related to the structural changes by alkali treatment, including acetyl hydrolysis, carboxyl deprotonation, absence of crystallization zone, and reduced inter- and intrachain entanglement. We believe that the good solubility and transparency of alkali-treated sphingan WL gum will help to promote its postmodification and application. This work is a good forerunner to studying the chain structure (conformation or helix, for instance) of sphingan WL gum.

## ASSOCIATED CONTENT

### Supporting Information

The Supporting Information is available free of charge at <https://pubs.acs.org/doi/10.1021/acsomega.3c00172>.

FTIR spectra of the samples with fixed alkali concentration (0.9 M NaOH) and different stirring times; <sup>1</sup>H NMR spectra (400 MHz) of sphingan WL gum (WL) and 0.9 M NaOH-treated WL (WL-0.9) in DMSO-*d*<sub>6</sub>; the standard curve of the acetyl group; the standard curve of glucuronic acid; XRD patterns of the samples with fixed alkali concentration (0.9 M NaOH) and different stirring times; AFM images of sphingan WL gum (WL) (A) and 0.9 M NaOH-treated WL (WL-0.9) (B) at 0.1 mg/mL; chain heights and diameters of sphingan WL gum (WL) and 0.9 M NaOH-treated WL (WL-0.9) and the chain lengths of WL-0.9 from AFM images (PDF)

## AUTHOR INFORMATION

### Corresponding Authors

Aiping Chang – *Fujian-Taiwan Science and Technology Cooperation Base of Biomedical Materials and Tissue*

*Engineering, Engineering Research Center of Industrial Biocatalysis, Key Laboratory of OptoElectronic Science and Technology for Medicine of Ministry of Education, College of Chemistry and Materials Science, Fujian Normal University, Fuzhou 350007 Fujian, China; Phone: +86-591-83465326; Email: aipingchang@fjnu.edu.cn; Fax: +86-591-83465326*

Hu Zhu – *Fujian-Taiwan Science and Technology Cooperation Base of Biomedical Materials and Tissue Engineering, Engineering Research Center of Industrial Biocatalysis, Key Laboratory of OptoElectronic Science and Technology for Medicine of Ministry of Education, College of Chemistry and Materials Science, Fujian Normal University, Fuzhou 350007 Fujian, China; [orcid.org/0000-0002-8359-3758](https://orcid.org/0000-0002-8359-3758); Phone: +86-591-83465326; Email: zhuhu@fjnu.edu.cn; Fax: +86-591-83465326*

## Authors

Jieying Lin – *Fujian-Taiwan Science and Technology Cooperation Base of Biomedical Materials and Tissue Engineering, Engineering Research Center of Industrial Biocatalysis, Key Laboratory of OptoElectronic Science and Technology for Medicine of Ministry of Education, College of Chemistry and Materials Science, Fujian Normal University, Fuzhou 350007 Fujian, China*

Jinfeng Deng – *Fujian-Taiwan Science and Technology Cooperation Base of Biomedical Materials and Tissue Engineering, Engineering Research Center of Industrial Biocatalysis, Key Laboratory of OptoElectronic Science and Technology for Medicine of Ministry of Education, College of Chemistry and Materials Science, Fujian Normal University, Fuzhou 350007 Fujian, China*

Zhenyin Huang – *Fujian-Taiwan Science and Technology Cooperation Base of Biomedical Materials and Tissue Engineering, Engineering Research Center of Industrial Biocatalysis, Key Laboratory of OptoElectronic Science and Technology for Medicine of Ministry of Education, College of Chemistry and Materials Science, Fujian Normal University, Fuzhou 350007 Fujian, China*

Hanyu Dong – *Fujian-Taiwan Science and Technology Cooperation Base of Biomedical Materials and Tissue Engineering, Engineering Research Center of Industrial Biocatalysis, Key Laboratory of OptoElectronic Science and Technology for Medicine of Ministry of Education, College of Chemistry and Materials Science, Fujian Normal University, Fuzhou 350007 Fujian, China*

Complete contact information is available at:

<https://pubs.acs.org/doi/10.1021/acsomega.3c00172>

## Author Contributions

Hu Zhu and Aiping Chang: conceptualization. Jieying Lin and Aiping Chang: investigation and writing-original draft. Jinfeng Deng, Zhenyin Huang, Hanyu Dong: data curation. Hu Zhu and Aiping Chang: writing-review and editing. All authors have read and agreed to the published version of the manuscript.

## Notes

The authors declare no competing financial interest.

## ACKNOWLEDGMENTS

This work was financially supported by the Natural Science Foundation of China (U1805234 and 22007013), Fujian-Taiwan Science and Technology Cooperation Base of Biomedical Materials and Tissue Engineering (2021D039),

Natural Science Foundation of Fujian Province of China (2020J05033), Program for Innovative Research Team in Science and Technology in Fujian Province University, 100 Talents Program of Fujian Province, Special Funds of the Central Government Guiding Local Science and Technology Development (2020L3008), and Scientific Research Start-up Fund for High-Level Talents in Fujian Normal University.

## ABBREVIATIONS

sphingan WL gum, WL; Fourier transforms infrared spectroscopy, FTIR; nuclear magnetic resonance, NMR; X-ray diffraction, XRD; dynamic light scattering, DLS; gel permeation chromatography, GPC; atomic force microscope, AFM

## REFERENCES

- (1) Guo, M. Q.; Hu, X.; Wang, C.; Ai, L. Polysaccharides: structure and solubility. In *Solubility of Polysaccharides*, Xu, Z., Ed.; IntechOpen, 2017; pp 7–21.
- (2) Klemm, D.; Heublein, B.; Fink, H.-P.; Bohn, A. Cellulose: fascinating biopolymer and sustainable raw material. *Angew. Chem., Int. Ed.* **2005**, *44* (22), 3358–3393.
- (3) Verbeken, D.; Dierckx, S.; Dewettinck, K. Exudate gums: occurrence, production, and applications. *Appl. Microbiol. Biotechnol.* **2003**, *63* (1), 10–21.
- (4) Li, H.; Jiao, X.; Sun, Y.; Sun, S.; Feng, Z.; Zhou, W.; Zhu, H. The preparation and characterization of a novel sphingan WL from marine *Sphingomonas* sp. *WG. Sci. Rep.* **2016**, *6*, 37899.
- (5) Li, H.; Feng, Z.-M.; Sun, Y.-J.; Zhou, W.-L.; Jiao, X.; Zhu, H. Draft genome sequence of *Sphingomonas* sp. WG, a welan gum-producing strain. *Genome Announc.* **2016**, *4* (1), e01709–15.
- (6) Kaur, V.; Bera, M. B.; Panesar, P. S.; Kumar, H.; Kennedy, J. F. Welan gum: Microbial production, characterization, and applications. *Int. J. Biol. Macromol.* **2014**, *65*, 454–461.
- (7) Jansson, P. E.; Lindberg, B.; Widmalm, G.; Sandford, P. A. Structural studies of an extracellular polysaccharide (S-130) elaborated by *Alcaligenes* ATCC 31555. *Carbohydr. Res.* **1985**, *139*, 217.
- (8) Ji, S.; Li, H.; Wang, G.; Lu, T.; Ma, W.; Wang, J.; Zhu, H.; Xu, H. Rheological behaviors of a novel exopolysaccharide produced by *Sphingomonas* WG and the potential application in enhanced oil recovery. *Int. J. Biol. Macromol.* **2020**, *162*, 1816–1824.
- (9) Chang, A.; Ye, Z.; Ye, Z.; Deng, J.; Lin, J.; Wu, C.; Zhu, H. Citric acid crosslinked sphingan WL gum hydrogel films supported ciprofloxacin for potential wound dressing application. *Carbohydr. Polym.* **2022**, *291*, 119520.
- (10) Li, B.; Li, H.; Liu, J.; Zhang, Z.; Chen, M.; Yue, L.; Lu, W.; Ji, S.; Wang, D.; Zhu, H.; Wang, J. Enzymatic degradation, antioxidant and rheological properties of a sphingan WL gum from *Sphingomonas* sp. WG. *Int. J. Biol. Macromol.* **2022**, *210*, 622–629.
- (11) Ruthes, A. C.; Smiderle, F. R.; Iacomini, M. D-Glucans from edible mushrooms: a review on the extraction, purification and chemical characterization approaches. *Carbohydr. Polym.* **2015**, *117*, 753–761.
- (12) Laszkiewicz, B. Solubility of bacterial cellulose and its structural properties. *J. Appl. Polym. Sci.* **1998**, *67* (11), 1871–1876.
- (13) Cai, J.; Zhang, L. Rapid dissolution of cellulose in LiOH/urea and NaOH/urea aqueous solutions. *Macromol. Biosci.* **2005**, *5* (6), 539–548.
- (14) Riaz, T.; Iqbal, M. W.; Jiang, B.; Chen, J. A review of the enzymatic, physical, and chemical modification techniques of xanthan gum. *Int. J. Biol. Macromol.* **2021**, *186*, 472–489.
- (15) Tako, M.; Teruya, T.; Tamaki, Y.; Konishi, T. Molecular origin for rheological characteristics of native gellan gum. *Colloid Polym. Sci.* **2009**, *287* (12), 1445–1454.
- (16) Alves, N. M.; Mano, J. F. Chitosan derivatives obtained by chemical modifications for biomedical and environmental applications. *Int. J. Biol. Macromol.* **2008**, *43* (5), 401–414.
- (17) Chen, Q.; Qi, Y.; Jiang, Y.; Quan, W.; Luo, H.; Wu, K.; Li, S.; Ouyang, Q. Progress in research of chitosan chemical modification technologies and their applications. *Mar. Drugs* **2022**, *20* (8), 536.
- (18) Bitter, T.; Muir, H. M. A modified uronic acid carbazole reaction. *Anal. Biochem.* **1962**, *4*, 330.
- (19) McComb, E. A.; McCready, R. M. Determination of acetyl in pectin and in acetylated carbohydrate polymers. hydroxamic acid reaction. *Anal. Chem.* **1957**, *29*, 819.
- (20) Hestrin, S. The reaction of acetylcholine and other carboxylic acid derivatives with hydroxylamine, and its analytical application. *J. Biol. Chem.* **1949**, *180* (1), 249–261.
- (21) Lodge, T. P.; Muthukumar, M. Physical chemistry of polymers: entropy, interactions, and dynamics. *J. Phys. Chem.* **1996**, *100* (31), 13275–13292.
- (22) Wang, L.; Xiang, D.; Li, C.; Zhang, W.; Bai, X. Effects of deacetylation on properties and conformation of xanthan gum. *J. Mol. Liq.* **2022**, *345*, 117009.
- (23) Chakka, V. P.; Zhou, T. Carboxymethylation of polysaccharides: synthesis and bioactivities. *Int. J. Biol. Macromol.* **2020**, *165* (Part B), 2425–2431.
- (24) Bao, D.; Chen, M.; Wang, H.; Wang, J.; Liu, C.; Sun, R. Preparation and characterization of double crosslinked hydrogel films from carboxymethylchitosan and carboxymethylcellulose. *Carbohydr. Polym.* **2014**, *110*, 113–120.
- (25) Kaur, J.; Kaur, G. Optimization of pH conditions and characterization of polyelectrolyte complexes between gellan gum and cationic guar gum. *Polym. Adv. Technol.* **2018**, *29* (12), 3035–3048.
- (26) Hassan, P. A.; Rana, S.; Verma, G. Making sense of brownian motion: colloid characterization by dynamic light scattering. *Langmuir* **2015**, *31* (1), 3–12.
- (27) Pal, N.; Verma, S. D.; Singh, M. K.; Sen, S. Fluorescence correlation spectroscopy: an efficient tool for measuring size, size-distribution and polydispersity of microemulsion droplets in solution. *Anal. Chem. (Washington, DC, U. S.)* **2011**, *83* (20), 7736–7744.
- (28) Fang, Y.; Duan, B.; Lu, A.; Liu, M.; Liu, H.; Xu, X.; Zhang, L. Intermolecular interaction and the extended wormlike chain conformation of chitin in NaOH/Urea aqueous solution. *Biomacromolecules* **2015**, *16* (4), 1410–1417.
- (29) Wang, X.; Xu, X.; Zhang, L. Thermally induced conformation transition of triple-helical lentinan in NaCl aqueous solution. *J. Phys. Chem. B* **2008**, *112* (33), 10343–10351.
- (30) Moffat, J.; Morris, V. J.; Al-Assaf, S.; Gunning, A. P. Visualisation of xanthan conformation by atomic force microscopy. *Carbohydr. Polym.* **2016**, *148*, 380–389.
- (31) Meng, Y.; Lyu, F.; Xu, X.; Zhang, L. Recent advances in chain conformation and bioactivities of triple-helix polysaccharides. *Biomacromolecules* **2020**, *21* (5), 1653–1677.
- (32) Cross, M. M. Rheology of non-Newtonian fluids: a new flow equation for pseudoplastic systems. *J. Colloid Sci.* **1965**, *20* (5), 417.
- (33) Zhong, L.; Oostrom, M.; Truex, M. J.; Vermeul, V. R.; Szecsody, J. E. Rheological behavior of xanthan gum solution related to shear thinning fluid delivery for subsurface remediation. *J. Hazard. Mater.* **2013**, *244–245*, 160–170.
- (34) Doi, M. Explanation for the 3.4 power law of viscosity of polymeric liquids on the basis of the tube model. *J. Polym. Sci., Polym. Lett. Ed.* **1981**, *19* (5), 265.
- (35) Ng, T. S. K.; McKinley, G. H. Power law gels at finite strains: the nonlinear rheology of gluten gels. *J. Rheol. (Melville, NY, U. S.)* **2008**, *52* (2), 417–449.
- (36) Ji, S.; Li, H.; Xue, H.; Guo, Z.; Liu, J.; Chen, M.; Wang, J.; Zhu, H.; Xu, H. Effects of monosaccharide composition and acetyl content on the rheological properties of sphingan WL. *Colloids Surf., A* **2022**, *650*, 129609.
- (37) Ramazani-Harandi, M. J.; Zohuriaan-Mehr, M. J.; Yousefi, A. A.; Ershad-Langroudi, A.; Kabiri, K. Rheological determination of the swollen gel strength of superabsorbent polymer hydrogels. *Polym. Test.* **2006**, *25* (4), 470–474.

(38) Van Den Bulcke, A. I.; Bogdanov, B.; De Rooze, N.; Schacht, E. H.; Cornelissen, M.; Berghmans, H. Structural and rheological properties of methacrylamide modified gelatin hydrogels. *Biomacromolecules* **2000**, *1* (1), 31–38.